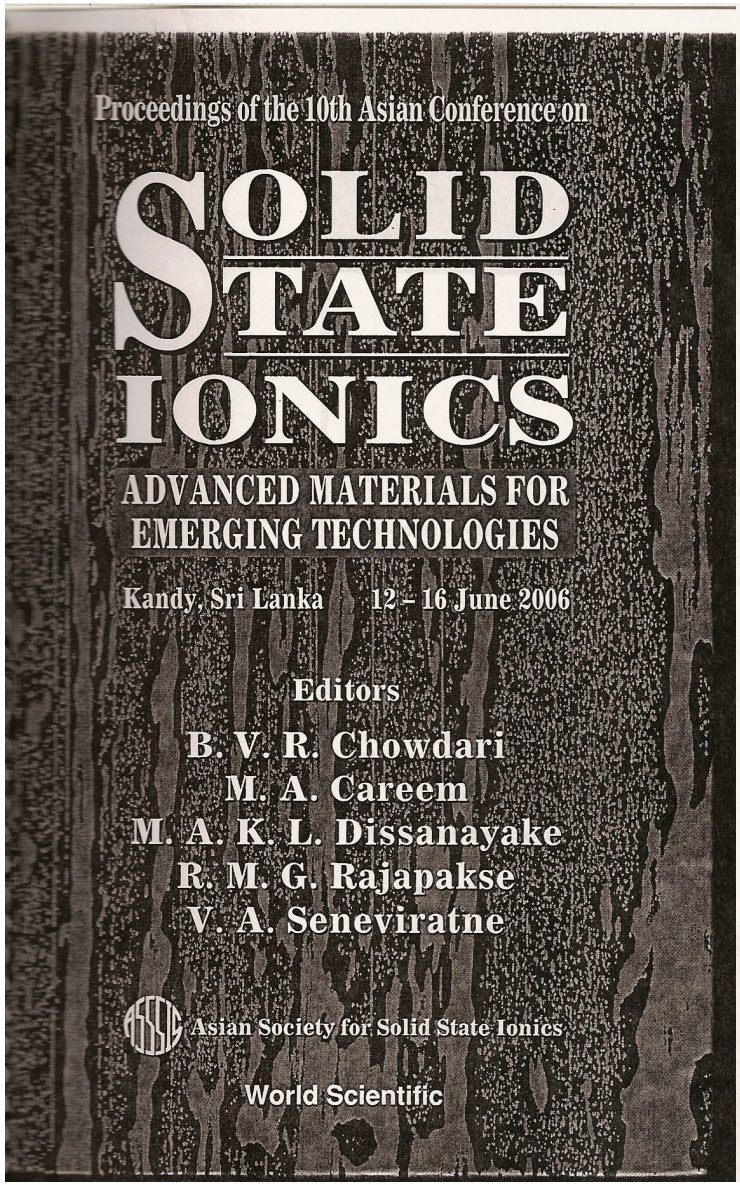

LAYERED ION-ELECTRON CONDUCTING MATERIALS

M.A. SANTA ANA, E. BENAVENTE, G. GONZÁLEZ*
Department of Chemistry, Faculty of Sciences, Universidad de Chile, Las Palmeras 3425, Santiago, Chile
Department of Chemistry, Universidad Tecnológica Metropolitana, Avenida Joé Pedro Alessandri 1242, Santiago, Chile.

Introduction

The characteristics of a given electrochemical device are essentially determined by the properties of the electrochemical cells defining its functionality. Any attempt directed to modify or regulate the characteristics of the device require an adequate selection of the materials used as electrodes and/or electrolytes.

The performance of an electrochemical cell is essentially determined by both, the activity of the electroactive species and its diffusion rate between the electrodes and, in the case of the electrodes, also by its electrical conductivity. The improvement of electrode materials implies therefore to optimize or regulate these variables according to the projected cell or device requirements.

In this work we describe selected features from the intercalation chemistry of the molybdenum disulfide analyzing the synthesis, characterization and properties of a series of organic-inorganic nanocomposites arising from the co-intercalation of organic donors and lithium into the sulfide. The conversion of some of these nanocomposites into functionalized nanotubes is also commented.

Layered Materials

There are a variety of chemical species which present stable laminar structures under normal conditions. This layered compounds are solids formed by pilling up planar or near planar layers. The stacking of the layers, extended along distances farther away than the typical bond distances, leads to characteristic highly anisotropic nanostructured arrangements. While the layers in these solids are constituted by relatively strong ionic-covalent interatomic interactions (150-300 kj/mol), showing electronic structures which may be described by typical electronic bands schemes, interactions between the layers are much weaker, frequently in the range 40-150 kj/mol[1]. Typical examples of these solids are those listed in Table 1.

Table1. Typical Layered Solids

Examples of Layered Solids	Layer Electronic Structure Nature	Electronic Conductivity (Scm^{-1})
Graphite	Metallic conductor	10^{-4} - 10^{3}
MoS_2, V_2O_5	Semiconductors	10^{-4}-10^{-6}
Synthetic and Natural Clays	Isolators	$< 10^{-12}$

One important and rather general feature in the chemistry of layered compounds is the insertion of chemical species in their interlamellar spaces leading to host-guest

compounds in which the inorganic matrix results functionalized by the inserted species[1,2,3].

Lithium intercalation compounds

A typical and widely known example of such functionalization processes is the intercalation of electron donors like alkali metals. Layered compounds are in general good candidates as materials for electrodes because of its capacity of hosting in the interlamellar spaces appreciable amounts of electroactive species with relatively large diffusion rates. Cobalt and nickel oxides as well as graphite, used respectively as negative and positive electrodes in rechargeable lithium batteries, are relevant examples of these materials[4]. The intercalation of lithium into MoS_2 may be performed chemically by reaction with butyl-lithium as well as by electrochemical reactions using appropriated cells like, for instance, $Au/Li/Li^+(solv)/MoS_2/Au$[5].

Although intercalation processes are generally considered to be topotactic, in the case of the MoS_2 important structural changes are apparent. The coordination of molybdenum by sulfur atom changes from trigonal prismatic in the pristine MoS_2 to an octahedral modification when it is intercalated, thus altering its band structure, changing its electronic conductivity, and promoting further intercalation processes [6,7].

Organic-Inorganic Nanocomposites

Lamellar inorganic matrices may be also intercalated by a variety of organic species leading to host-guest nanocomposites. The intercalation reaction is often an spontaneous process performed under rather mild conditions which may be seen as resulting from the molecular recognition between the organic and the inorganic components. Thus, these lamellar nanoheterogeneous species appear to be the transition between a composite and a conventional compound. Because of the number of possible combinations leading to products with slightly different properties, this approach may be useful for the design of tailor-made materials.

Co-Intercalation of Lithium and Organic Donors into Molybdenum Disulfide

The intercalation of organic species into MoS_2 requires an activation step, which frequently consists in the intercalation of lithium (*ca.* one mole per mol MoS_2) followed of a rapid hydrolysis of the product. There, factors like a light increase in electron charge in the host, the conversion of the trigonal prismatic 2D MoS_2 into the octahedral 1T modification, and the exfoliation of the lamellar solid promote the intercalation of donors in this host[8].

	H_2O		Organic	
Li_xMoS_2 (s)	→	**$Li_x(H_2O)_nMoS_2$ (susp.)**	→	**$Li_xMoS_2(D)_y$**
x≈1		x≈0.1	Donor	x≈0.01-0.3, y=0.1-2.5
Δc= 6.14 Å		Δc= 11.4 Å		Δc= 8-50 Å

The intercalation of organic species causes important changes of the interlamellar spaces. As illustrated in Fig.1, these changes may be easily followed by powder X-ray diffraction analysis of the products. Since in lamellar compounds the intensity of the *00l* reflections are abnormally enhanced, the purity of the products as well as the interlamellar distances may be straightforward determined.

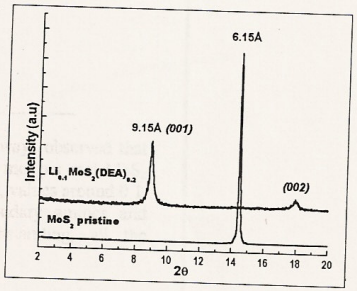

Figure 1. X-ray diffraction pattern of the MoS_2 and $Li_{0.1}MoS_2(DEA)_{0.2}$

In Table 2 are reported selected examples of MoS_2-based nanocomposites obtained by chemical methods. All of them corresponds to pure phases with characteristic stoichiometries and interlamellar distances showing well defined lamellar microstructures . Using simple molecular models for the guest species, it is always possible to corroborate, using geometric criteria, that the structural and analytical characteristic of the compounds agree with the volume in the interlamellar space and the surface on the host molecular sheets respectively[9].

Tables 2. Interlamellar distances of MoS_2-based nanocomposites

Compound*	Interlamellar distances Å
$Li_{0.1}MoS_2(DEA)_{0.4}$	9.8
$Li_{0.1}MoS_2(DBA)_{0.2}$	10.5
$Li_{0.1}MoS_2(PEO)_{0.5}$	11.0
$Li_{0.1}MoS_2(PEO)_{1.0}$	16.0
$Li_{0.1}MoS_2(PAN)_{1.1}$	11.5
$Li_{0.32}MoS_2(12\text{-Crown-4})_{0.2}$	14.0

* DEA: diethyamine; DBA: dibuthylamine ; PEO: polyethylene oxide; PAN: polyacrylonitrile

Changes are however not only limited to the interlamellar distances and stoichiometries. Electrical and electrochemical properties of the products differ

from those of the components. In some cases the structure of the intercalated donor from different from that in the free state

Electrical and ionic conductivity

The electrical conductivity of the intercalation products results in most cases to be considerably higher than that of the pristine MoS_2. As observe in Table 3, it strongly depends on the nature of the intercalated donor. The dependence of the conductivity on the temperature generally shows linear Arrhenius plots in the near room temperature range, increasing steady with the temperature.

Tabla 3 Electrical conductivity of MoS_2 and MoS_2 - donor nanocomposites

Compound	Electrical conductivity σ (298 K) (S cm^{-1})
$Li_{0.1}MoS_2(PEO)_{0.5}$	4.80×10^{-4}
$Li_{0.1}MoS_2(PEO)_{1.0}$	6.60×10^{-3}
$Li_{0.1}MoS_2(PEO)1.4$	1.04×10^{-2}
$Li_{0.2}MoS_2(DEA)_{0.42}$	2.51×10^{-1}
$Li_{0.1}MoS_2(DBA)_{0.19}$	1.97×10^{-1}
$Li_{0.1}MoS_2(Diciclohexylamine)_{0.07}$	3.80×10^{-2}
$Li_{0.32}MoS_2(12\text{-}Crown\text{-}4)_{0.2}$	8.50×10^{-2}
$Li_{0.6}MoS_2\ (PAN)_{1.2}$	3.30×10^{-4}
MoS_2	2.09×10^{-6}

In the intercalation of organic electron-pair donors it is always observed that the products contain lithium in an amount in the range 0.1-0.6 mol per mol MoS_2 depending on the nature of the organic donor. Thus, for instance, values around 0.1, 0.2 and 0.6 in the intercalation of linear polyethers, secondary amines and polyacrylonitrile are respectively observed. That not withstanding, all the compounds behave as mixed ionic-electronic conductors[10].

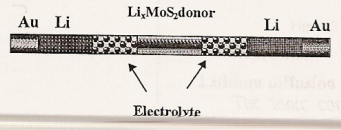

Although in these compounds the electron conductivity contribution is expected to be many orders of magnitude higher than that of the ionic conductivity, the separation of both contributions may be afforded by galvanostatic polarization-measurements using the cell schematized in Fig 2. Results of a polarization experiment for the compound $Li_{0.1}MoS_2(DBA)_{0.19}$ are shown In Fig.3. As expected the ratio between both contributions is about 10^5 [11].

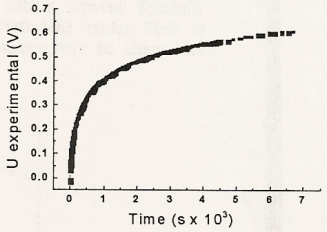

Figure 3.Galvanostatic polarization for the compound $Li_{0.1}MoS_2(DBA)_{0.19}$. Constant current density j = 8μA ·cm^{-1}.

Lithium diffusion coefficients

The ionic conductivity observed in these compounds is associated to the lithium located in the interlamellar phase, so they are a measure of the mobility of the lithium species in this phase. However, in order to asses the quality of the products as eventual electrode materials for electrochemical devices, the lithium diffusion coefficients appears to be more realistic than the ionic conductivity for analyzing the transport of lithium across a given phase.

Lithium diffusion coefficients may be obtained by following the rate at which lithium, deposited on the tested electrode by a short current pulse left the surface for diffusing in the bulk of the material. If the measurements are carried out at different lithium contents and different temperatures, a picture of the macroscopic movement of lithium across the solid may be obtained.

In Table 4 are reported the diffusion coefficients determined for a selected series of nanocomposites intercalated with different organic donors measured under comparable temperature and lithium content conditions. This variable clearly depends on the nature of the interlamellar phase, not only on the organic functional group of the guest but also on the stoichiometry of the phase. There is not any clear relationship between the interlamellar distances in the nanocomposite, the donor ability of the guest or any other characteristic of the products. This property appears to be determined by the particular molecular structure of the interlamellar phase each intercalate (vide infra) [10,12].

Table 4. Diffusion coeficients of Li in MoS_2 and in MoS_2-donor nanocomposites at 298 K.

COMPOUND	X = 0.2 D $cm^2 s^{-1}$	X = 0.4 D $cm^2 s^{-1}$	X = 0.5 D $cm^2 s^{-1}$
$Li_x MoS_2$ Pristine	$1.4\ 10^{-13}$	$4.2\ 10^{-14}$	$1.4\ 10^{-14}$
$Li_x MoS_2$ Restacked	$3.1\ 10^{-13}$	$4.64\ 10^{-14}$	$1.54\ 10^{-14}$
$Li_x MoS_2$ $(PEO)_1$	$1.0\ 10^{-12}$	$4.5\ 10^{-13}$	$2.6\ 10^{-13}$
$Li_x MoS_2$ $(PEO)_{0.5}$	$3.0\ 10^{-11}$	$1.0\ 10^{-12}$	$8.5\ 10^{-14}$
$Li_x MoS2$ $(PAN)_1$	$4.3\ 10^{-11}$	$5.8\ 10^{-12}$	$2.3\ 10^{-13}$ (x =0.6)
$Li_x MoS2$ $(NMCHA)_{0.4}$	$2.0\ 10^{-12}$	$1.42\ 10^{-12}$	$5.6\ 10^{-13}$ (x =0.6)
$Li_x MoS2$ ($DEA)_{0.3}$	$1.48\ 10^{-11}$	$1.7\ 10^{-12}$	-----

For the pristine MoS_2 as well as for all of its intercalation products tested in our laboratory, a near linear Arrhenius behavior is observed. In pure MoS_2 a lithium-ion hopping mechanism is apparent, what, as deduced from the constancy of the observed lithium diffusion activation enthalpy, is independent of the amount of intercalated lithium. In the case of lithium co-intercalated with organic donors, where the lithium species are expected to be surrounded not only by the matrix sulfur atoms but by the guest donor atoms (*vide infra*), the process is more complex. The slopes in the Arrhenius plots change with the lithium content. Specially interesting is the co-intercalation of lithium and poly(ethylene oxide), PEO, in which case two pure phases with different stoichiometry may be chemically afforded, $Li_{0.1}MoS_2(PEO)_{0.5}$ and $Li_{0.1}MoS_2(PEO)_{1.0}$.

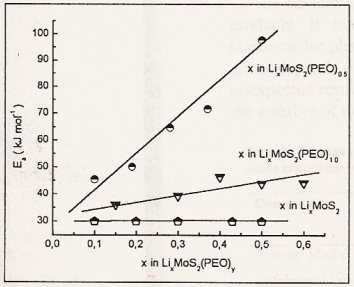

Figure 4. Diffusion activation enthalpy for MoS_2 and PEO-nanocomposites.

As observed in Fig. 4, slightly changes in the diffusion activation enthalpy occurs for the nanocomposites intercalated with one mol PEO per mol MoS_2 while for those containing 0.5 mol a much higher dependence is observed. A plausible explanation of these observations may be found, as discussed below, in the different structures of the interlamellar phase existing in these two products.

Electrochemical Lithium/Intercalated-Lithium Potentials

Using electrochemical cells similar to those described above, the electrochemical potential of the couple Li-metal/intercalated-Li in the products as prepared chemically as well as in those with different lithium intercalation degrees may be determined. Since electrochemical potentials correspond to the activity of the electroactive species, these measurements permit to investigate the effect of the different co-intercalated donors on the stabilization of the lithium ion in the interlamellar phase as well as on the capacity of the electrode and the variation of the potential in charge-discharge processes.

In Table 5 the average potentials observed for a selected series of intercalated products. It may be there observed, that the presence of the donor in the interlamellar phase clearly increases the lithium ion activity. The magnitude of this effect depends on the nature of the co-intercalated species. That is certainly not an unexpected result, since the Lewis-base nature of the organic guests should increase the stability of the lithium ion by coordinative interactions[13].

Tabla 5. Average quasi-equilibrium potentials for the intercalation of lithium in MoS_2 and MoS_2 – donor nanocomposites. Lithium concentration range: 0.2- 0.6 mol per mol compound.

Compound	Average Potential V (Li/Li^+)
Pristine MoS_2	1.60
Exfoliated MoS_2	1.64
$Li_x MoS_2$ $(PEO)_1$	2.61
$Li_x MoS_2$ $(PEO)_{0.5}$	2.78
$Li_x MoS_2$ $(PAN)_1$	2.84
$Li_x MoS_2$ $(DEA)_{0.2}$	2.80
$Li_x MoS_2$ (n-MCHA)$_{0.4}$	2.60

More instructive information than the average values in is obtained by analyzing the quasi-equilibrium lithium intercalation curves Some examples are displayed in Fig. 5. As observed, the variation of the potential with the lithium content also depends on the co-intercalated organic guest. Pure MoS_2 displays an extreme case of dependence. Lithium-ion activity strongly decreases with the amount of intercalated lithium. In other words, the metallic character of lithium in the intercalated phase increases significantly along the discharge. These results agree with some XPS experiments performed with the compound $Li_{0.8}MoS_2$ which, as deduced from results observed in Table.6 show that lithium in these compounds displays a behavior more like the metallic lithium than other lithium compounds [14].Clearly in these intercalates host-guest charge transfer is rather incomplete

affecting the electrode capacity. This partial charge transfer has been also deduced from theoretical calculation made for this and other similar compounds[15].

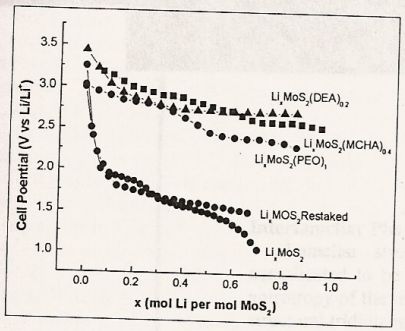

Figure 5. Variation of the quasi-equilibrium potential with the lithium content along the intercalation of lithium into MoS_2 pure and modified by the co-intercalation of donors.

Tabla 6. Binding energies of Li(1s)

Compound	E_b eV
$LiBF_4$	59.9
LiCl	58.1
LiBr	56.8
$LiNH_2$	55.8
Li MoS_2	55.6
Li(metal)	55.5

Contrasting with the experiments already discussed, the presence of some intercalate does not only enhance the lithium-ion activity but also permits the incorporation of a higher amount of lithium without major detriment to the cell potential, thus increasing its capacity. However, such an effect is different for each nanocomposite. The explanation may be not always found in an increment of the lithium-host charge transfer since the later has certainly a limit which should be not much higher than that observed for the MoS_2 alone. Probably, that is also related to the state of lithium in the interlamellar phase, which in some cases like in the intercalation of amines, are able to form aggregates (*vide infra*) [16].

Interlamellar Phase Structure

Lamellar structures like those analyzed in this work are intrinsically complicated to be studied by precise crystallographic methods. Due to the high anisotropy of the interactions involved in their constitution, they often shows a low structural tridimensional coherence. That is specially valid for the organic-inorganic nanocomposites in which the organic phase presents a high mobility resembling more a liquid than a solid phase. The structure of the interlamellar phase has to be studied by indirect methods like wide-line nuclear magnetic resonance spectroscopy at variable temperature. In the case of the nanocomposites formed by the co-intercalation of lithium and donor species discussed here, ^{7}Li-NMR studies provide interesting information about the relative position of the lithium atoms in the interlamellar phase. The ^{7}Li-^{7}Li and ^{7}Li-^{1}H second magnetic moments, calculated from the resonance line half high width in the ^{1}H-coupled and decoupled ^{7}Li-spectra at low temperatures (rigid state) permit to determinate by comparison with suitable molecular models both the relative positions of the lithium atoms and the distances between them and the neighboring hydrogen atoms. These studies, limited at the moment to the nanocomposites with poly(ethylene oxide) and secondary amines, show that in the confined state not only the inorganic matrix undergoes changes but also both, lithium and the donors may present conformations different from those in the free state [17].

As shown schematically in Fig. 6 in the PEO derivatives $Li_{0.1}MoS_2(PEO)_{0.5}$ and $Li_{0.1}MoS_2(PEO)_{1.0}$ with second magnetic moments $M_2(^7Li\text{-}^7Li)$ of 0.014 and 0.050 G^2 respectively, lithium is found coordinated by the polymer oxygen atoms and distributed in a form practically homogenous in the phase. There are however important differences between these nanocompostes. In $Li_{0.1}MoS_2(PEO)_{0.5}$ the interlamellar phase is formed by one polymer layer where lithium is simultaneously coordinated by the polymer and the host sulfur atoms. Meanwhile in $Li_{0.1}MoS_2(PEO)_{1.0}$ where a polymer bilayer is apparent, the lithium atoms are totally surrounded by the polyether oxygen atoms. Moreover, the conformation of the polymer in both cases, a zig-zag conformation in the former and TGG arrangement in the latter differs from the helical conformation, characteristic of the free polymer.

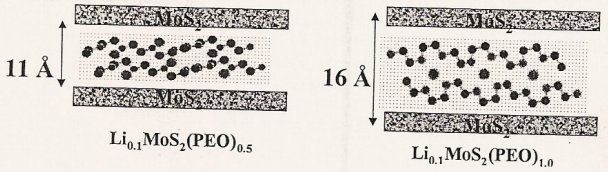

Figure 6. .Schematic representation of the conformation of POE in the MoS_2 interlaminas spaces $Li_{0.1}MoS_2(PEO)_{0.5}$ and $Li_{0.1}MoS_2(PEO)_{1.0}$

These results agree well with the lithium diffusion coefficient studies commented above. In the case of $Li_{0.1}MoS_2(PEO)_{1.0}$ with the lithium in an homogeneous oxygen coordination cage, the diffusion activation enthalpies show

only an small dependence on the lithium intercalation degree. Contrastingly in the compound $Li_{0.1}MoS_2(PEO)_{0.5}$ where there is a mixed coordination around lithium, the changes produced by lithium intercalation are notoriously more drastic (Fig. 4) [18].

Since the MoS_2/amine intercalates show in general relatively high Li/Li^+ potentials, electrical conductivities and lithium diffusion coefficients, it was specially interesting to analyze the state of lithium in the interlamellar phase of these nanocomposites. The ^7Li-^7Li second magnetic moments obtained from the ^7Li-NMR spectra result to be surprisingly high, in a range 1.3-1.6 G^2 [17]. This data reveals that in this compounds there is an agglomeration of lithium atoms. Using simple molecular models it is possible to deduce that observed Li-Li interactions corresponds to the formation of lithium metal clusters. In diethylamine a trinuclear species is stabilized, while for the di-butyl and di-pentyl derivatives the formation of tetranuclear aggregates is observed. The tendency of lithium to form aggregates is well known in lithium, however the three-nuclear as well as the stabilization of Li cluster by secondary amines is somewhat surprisingly. The role of the amine in these intercalates appears to be the formation of a coordination cage around the cluster, showing a pseudo-micellar behavior. Although the latter is common for long chain derivatives, it has been not observed before for small amines. Thus, the behavior of both lithium and amine in these nanocomposites appears to be induced by confinement effects.

The peculiar arrangement of the components of the interlamellar phase should have a marked influence on both the thermodynamics and kinetics of lithium in these compounds, thus bearing to special electrical and electrochemical properties.

Conversion of Lamellar Nancomposites into Tubular Structures

Finally it is interesting to comment the possibility of obtaining one dimensional objects, specifically nanotubes, starting from lamellar organic-inorganic nanocomposites similar to those commented above.

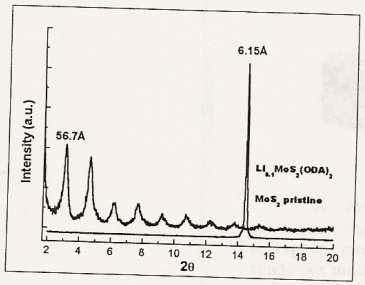

Figure 7. X-ray diffraction pattern of the MoS_2 and $Li_{0.1}MoS_2$(octadecylamine)$_2$

The intercalation of long chain amines into MoS_2 leads to high ordered laminar structures (Fig 7). Such a regular arrangements in the perpendicular direction to the molecular MoS_2 planes is possibly due to cooperative effects caused by the self-assembling of the amphiphilic organic donors, which indeed, are found forming organic bilayers in the host interlamellar spaces.

The treatment of these products under hydrothermal conditions *i.e.* temperature in the range 100-150 °C and auto-generated pressures, leads to multiwall MoS_2 nanotubes, which retain in the interlamellar spaces the organic donor. Selected images of these products are shown in Fig.8 [19].

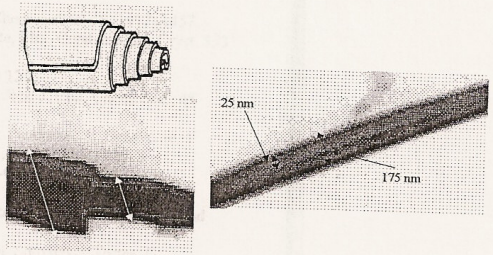

Figure 8. TEM image of MoS_2 nantotubes.

As observed in the figures, these nanotubes displaying a multilayer constitution appear to be generated from the lamellar intercalated precursors by a rolling up process. Such a mechanism, rather plausible given the reaction conditions much softer than those normally used for generating carbon nanotubes and inorganic fullerenes, appears to be also valid for other nanocomposites. Indeed, many V_2O_5-based functionalized tubular structures have been prepared using this method. Although experiments performed until now are limited to lamellar matrices intercalated with long chain amines, we think that other structurally similar organic-inorganic nanocomposites may be also prepared either directly by rolling up bi-dimensional precursors or by exchanging the donors from the interlamellar spaces. The benefits associated to the high anisotropic electrical and electrochemical behavior expected for one dimensional structures encourage further research in this field.

Conclusions

The lamellar MoS_2-based organic-inorganic nanocomposites described in this work show electrical and electrochemical properties which, from the point of view of its use as electrode in electrochemical devices, are better than the pristine inorganic sulfide. The relative easy methods used for the preparation of these nanocomposites and, specially, the dependence of their properties on the nature of

the organic donor co-intercalated with lithium make these products interesting in the design of electrode materials with predetermined electrochemical properties. Moreover, the intrinsic anisotropy of the products open the possibility of their utilization in intelligent devices. The chance of converting these bidimensional laminar products in functionalized one dimensional tubular nanostructures enhances the interest in the chemistry of this kind of intercalation compounds.

Acknowledgements. Research partially founded by FONDECYT (Grant 1050344, 7050085, 1030102, 7050081), DI Universidad de Chile and Universidad Tecnológica Metropolitana.

References

1. D. O'Hare, D. W. Bruce, D. S. O'Hare (Eds), Inorganic Materials, Wiley, Chichester, 1992
2. E. P. Gianellis, Adv. Mater. 8 (1996) 1
3. R. Schöllhorn in: J. L. Atwood, J. E. D. Davies, D. D. MacNicol (Eds), Inclusion Compounds, vol 1, Academic Press, London, 1984 (chap. 7).
4. M. Winter, J. O. Besenhard, M. E. Spahr, P. Novák, Adv. Mater, 10 (1998) 725.
5. G. González, M. A. Santa Ana, E. Benavente, Electrochim. Acta, 43 (1998) 1327.
6. M. A. Py, R. R. Haering, Can, J. Phys. 61 (1983) 76.
7. E. Benavente, M. A. Santa Ana F. Mendizábal, G. González, Coord Chem Rew 224 (2002) 87 -109.
8. W. M. R. Divigalpitiya, R. F. Frindt, S. R. Morrison, J. Mater. Res., 6, (1991) 1103.
9. M. B. Dines, Science, 188 (1975) 1210.
10. M. A. Santa Ana, E. Benavente, G. González, J. Coord. Chem. 54 (2001) 481.
11. V. Sánchez, E. Benavente, M. A. Santa Ana, G. González, Chem. Mater. 11 (1999) 2296.
12. G. González, M. A. Santa Ana, E. Benavente, J. Phys. Chem. Solids, 58 (1997) 1457.
13. G. González, M. A. Santa Ana, V. Sánchez, E. Benavente, Mol. Cryst and Liq. Cryst. 353 (2000) 301.
14. G. González, H. Binder, Bol. Soc. Chil Quim. 41 (1996) 121
15. F. Mendizábal, M. A. Santa Ana, E. Benavente, G. González, J. Chil. Chem. Soc., 48 (2003) 69.
16. A. C. Bloise, J. P. Donoso, C. J. Magon, J. Schneider, H. Panepucci, E. Benavente, V. Sánchez, M. A. Santa Ana, G. González, J. Phys. Chem., B 106 (2002) 11698.
17. E. Benavente, M. A. Santa Ana, G. González, F. Becker-Guedes, N. C. Mello, H. C. Panepucci, T. J. Bonogamba, J. P. Donoso, Electrochim. Acta 48 (2003) 1997.
18. G. González, M. A. Santa Ana, E. Benavente, V. Sánchez, N. Mirabal, Mol. Cryst. and Liq. Cryst. 374 (2002) 229.
19. V. Lavayen, N. Mirabal, E. Benavente, J. Seekamp, C. M. Sotomayor Torres, G. González, in H. Kuzmany, J. Fink, M. Mehring, S. Roth (Eds). CP685, Molecular Nanostructures: XVII Int' l. Winterschool/Euroconference on Electronic Properties of Novel Materials, 2003, 473.